Rapid reconstruction of a strong nonlinear property by a multiple lock-in technique

Shigeki Kawai,[1,*] Sadik Hafizovic,[2] Thilo Glatzel,[1] Alexis Baratoff,[1] and Ernst Meyer[1]
[1]*Department of Physics, University of Basel, Klingelbergstrasse 82, 4056 Basel, Switzerland*
[2]*Zurich Instruments AG, Technoparkstrasse 1, 8005 Zurich, Switzerland*
(Received 17 December 2011; revised manuscript received 20 March 2012; published 13 April 2012)

We propose and discuss a rapid reconstruction procedure for strongly nonlinear signals and validate it for dynamic force microscopy. Harmonics of the cantilever resonance frequency shift, generated by a low-frequency modulation of the tip-sample distance, are detected by a phase-locked loop followed by 12 lock-in amplifiers. The distance dependence of the frequency shift can be reconstructed by summing up the sampled Fourier components with judiciously assigned phase shifts. Following a successful test with a model potential, we report a measurement of the frequency shifts induced by the force field above a KBr(001) surface at room temperature in ultrahigh vacuum. Experimental spectra justify the neglect of harmonics beyond tenth order in the range where clear atomic-scale contrast appears in images of the lower harmonic intensities. A high-resolution three-dimensional frequency shift dataset was measured in 400 s. The method can in general be applied to any single-valued physical quantity with a smooth nonlinear dependence on a control variable.

DOI: 10.1103/PhysRevB.85.165426 PACS number(s): 46.80.+j, 07.79.Lh, 34.20.Cf, 78.20.Bh

I. INTRODUCTION

Understanding potential energy variations on surfaces is of cardinal importance in controlling the growth and etching of crystals, adsorption,[1] and friction.[2] Since the first site-dependent dynamic force spectroscopy (DFS) on Si(111)-7×7 at low temperature (LT),[3] DFS has become a reliable tool for the detection of tip-sample interaction on the atomic scale. In DFS, the tip-sample Z distance is usually swept slowly while recording the frequency shift Δf of a cantilever flexural resonance. More precisely, first the tip-sample Z distance is kept constant and Δf is recorded for a certain time (typically $1 \sim 10$ ms); Z is then incremented to a smaller or larger value. By repeating this procedure, the distance dependence of Δf above a certain surface-site is measured. The force and potential energy extracted from the measured $\Delta f(Z)$ by numerical deconvolution provide detailed insights into the tip-sample interaction. Even surface species can be successfully discriminated by comparing the *relative* ratios of the maximum attractive interaction forces.[4]

This technique has recently been extended to high-resolution three-dimensional (3D)-DFS, and it has become an important tool in the study of tip-sample interaction forces, in spite of stochastic fluctuations causing energy dissipation.[5] Such 3D measurements have mainly been demonstrated at LT where thermal drifts are very small.[6–8] By incorporating atom-tracked tip-positioning to compensate thermal drifts,[9] high-resolution 3D-DFS measurements have very recently been demonstrated at room temperature (RT).[10] However, in both cases, the whole measurement usually takes more than 10 h due to the required enormous number of measurement points ($\sim 10^5$). Reducing the total measurement time is one of the most important objectives. Although a 3D-DFS measurement was successfully performed in a liquid cell in almost one minute with a specially designed high-speed microscope,[11] a common problem with sequential measurements is that the sweep rate falls in the range where $1/f$ noise dominates and spoils the linear relationship between noise power and bandwidth.[12] In order to increase the signal-to-noise ratio, the measurement bandwidth B is usually set narrow, thus averaging the Δf signal over a longer period. Thus, time-domain approaches commonly used in most physical measurements are intrinsically time-consuming.

This issue has been well-addressed and led to the widespread use of the lock-in detection technique for improving the signal-to-noise ratio by measuring the amplitude and phase of the synchronous response to an input signal at a modulation frequency in the range where the noise is white to a good approximation.[13] In dynamic force microscopy, several measurements of an additional quantity of interest recorded with a lock-in amplifier have previously been reported.[14,15] Their focus, however, has been on the detection of the first harmonic signal. One notable exception is intermodulation spectroscopy, which uses strong input signals at two (or more) fixed frequencies close to a resonance in order to extract the nonlinear dependence of, e.g., the tip-sample interaction force, from the amplitudes of many harmonics of the difference frequency excited around the resonance.[16,17] However, the narrow width of cantilever resonances, which is desirable for sensitive atomic-scale resolution measurements and is achieved in ultrahigh vacuum (UHV), would markedly reduce the number of observable harmonics and might also prevent stable operation. For this reason, such measurements rely on the sensitive frequency demodulation (FM) detection of small resonance frequency shifts,[18] instead of detecting amplitudes of signals excited at fixed frequencies.

In this article, we present a rapid reconstruction procedure for any quantity with a nonlinear dependence on a control variable and apply it to generate a 3D site-dependent Δf map. In contrast to time-domain measurements, the Δf signal is sampled above the $1/f$ noise range. Many harmonics are generated by modulating the tip-sample distance Z in a range where Δf is strongly nonlinear while the tip scans over a KBr(001) surface. Twelve individual harmonic signals detected by multiple lock-in amplifiers proved sufficient to reconstruct a 3D-Δf landscape with atomic resolution in 400 s at RT, 210 times faster than a similar recent drift-corrected time-domain measurement.[10]

II. THEORETICAL JUSTIFICATION

This novel approach was first validated by a simple numerical calculation. Figure 1(a) shows a typical distance dependence of the frequency shift calculated from $\Delta f(Z_c) = -f/\pi kA \int_0^\pi F[Z_c + A(1+\cos\theta)]\cos\theta d\theta$,[19] where A is the amplitude, k the mode stiffness, f the resonance frequency, F the force on the tip, and Z_c the lower turning point of the oscillation. The assumed force is based on the Morse potential for the short-range chemical Si-Si interaction[20] and a Hamaker-type long-range interaction[21] with the parameters used in Ref. 22. When the tip-sample Z distance is additionally modulated by applying a sinusoidal voltage to the sample Z scanner, the relative tip apex motion can be expressed as $Z(t) = Z_c + A_Z(1+\cos 2\pi f_Z t) + A(1+\cos 2\pi f t)$, where A_Z is the amplitude of the Z scanner modulation and f_Z its frequency. This motion is formally similar to that in bimodal DFM,[22–24] where two resonance frequencies (f_1, f_2) are tracked and excited, but higher harmonic, sum, and difference signals at frequencies $nf_1 \pm mf_2$, n and m being integers, are not detected in practice due to intentional bandpass filtering and to the limited frequency detection bandwidth B. However, in the present measurement, $f_Z = 30$ Hz is chosen much lower than B so that many frequency modulation sidebands of the cantilever resonance frequency can be detected without distortion within the window $f \pm B$. In other words, the scanner motion can be viewed as a slow modulation of $\Delta f(Z)$ sampled at $Z = Z_c + A_Z(1+\cos 2\pi f_Z t)$, approximately like when a conventional $\Delta f(Z)$ curve is recorded at a sweep rate much lower than f. Owing to the pronounced nonlinear distance dependence of Δf, the detected $\Delta f(t)$ signal in Fig. 1(b) contains many harmonics of f_Z, which can be clearly observed in the calculated fast Fourier transform (FFT) amplitudes in Fig. 1(c). The intensities R_i of the higher harmonics vary nonmonotonically but eventually drop exponentially with increasing order i. This behavior can be related to the distance dependence of various contributions to the underlying force $F(Z)$ by the following qualitative argument. Without modulation, the distance dependence of $\Delta f(Z)$ is qualitatively similar to that of $F(Z)$, apart from a small shift of the whole curve to the right of the force minimum for the small A assumed here. The observed behavior of R_i versus if_Z should, therefore, be similar to the dependence of the harmonics F_m of $F[Z(t)]$, which would be generated at

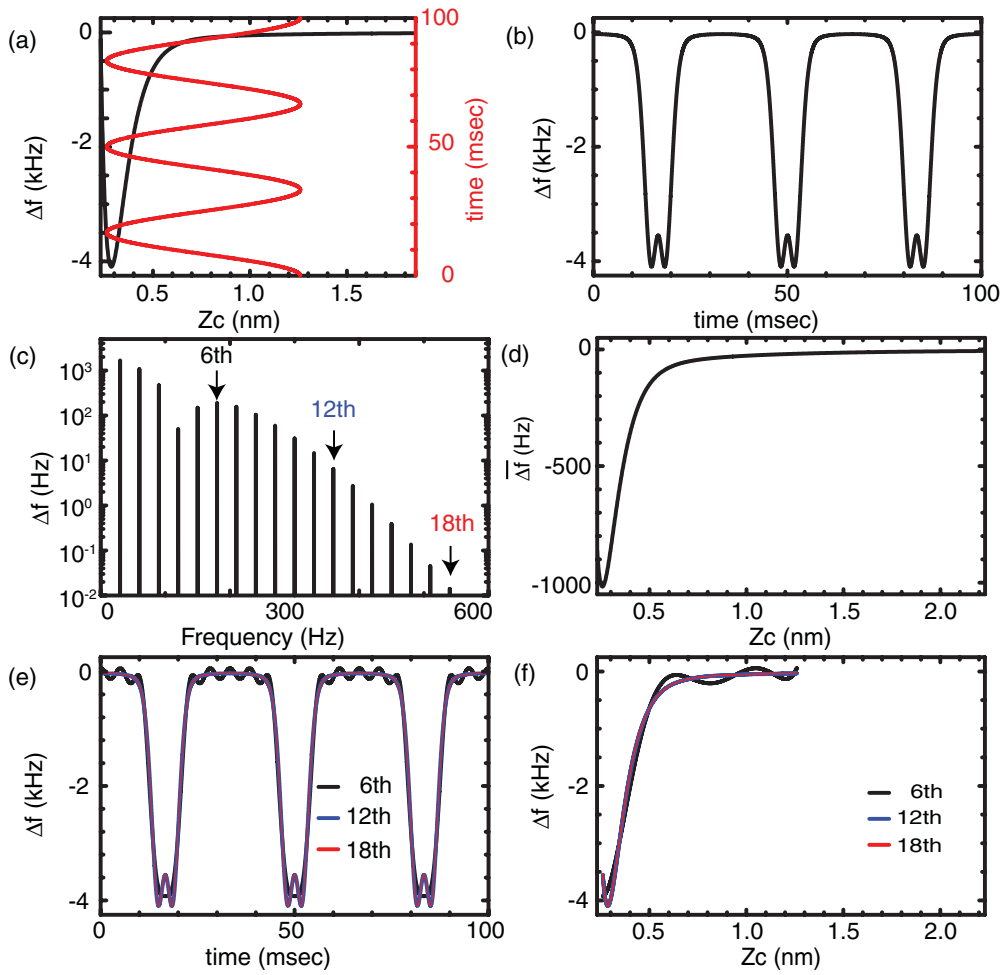

FIG. 1. (Color online) (a) Modeled distance dependence of the frequency shift Δf and real-time Z scanner modulation. (b) Δf signal in the time domain and (c) its fast Fourier transform amplitudes in the frequency domain. (d) Calculated distance dependence of the time-averaged Δf. (e) Reconstructed real-time Δf signals and (f) their distance dependencies, including up to 6, 12, and 18 harmonics. Calculation parameters: resonance frequency, $f = 1$ MHz; cantilever oscillation amplitude, $A = 100$ pm; effective mode stiffness, $k = 1400$ N/m; Z scanner modulation frequency, $f_Z = 30$ Hz; and amplitude, $A_Z = 500$ pm.

frequencies mf by a cantilever resonance oscillation with an amplitude $A = A_Z$, namely[25]

$$F_m = \frac{1}{\pi}\int_0^{\pi} F[Z_c + A(1+\cos m\theta)]\cos m\theta d\theta. \quad (1)$$

Such harmonics with $m > 1$ are seldom considered because the induced oscillations are not resonance enhanced. If $2A$ covers the range where $F(Z)$ varies strongly, while Z_c is within that range, Eq. (1) implies that F_m integrand begins to drop once the first zero crossing of $\cos m\theta$ near the turning point ($\theta = \pi$) falls within the range of $F[Z(\theta)]$. Expanding about the turning point and applying this argument to the different force components, one finds that the threshold m is roughly $\sqrt{A/\lambda}$. Here, $\lambda_a > \lambda_r$ are the decay lengths of the attractive and repulsive parts of the short-range force ($\lambda_a = 2\lambda_r$ for the assumed Morse interaction and $\lambda_a = 79$ pm used here for the Si-Si interaction[20]), whereas $\lambda = n/Z_c$ for a long-range force $\propto Z^{-n}$ ($n = 2$ for the Hamaker interaction with a spherical tip). A similar behavior is therefore expected in Fig. 1(c), when the modified criterion $i > C\sqrt{A_Z/\lambda}$, C being a constant of order unity depending on the particular force law, is satisfied for a particular component, whereby n should be replaced by $n - 1/2$, according to Ref. 21. In the time domain, $\sqrt{\lambda/A_Z}/f_Z$ is the analog of the short-range interaction time $\sqrt{\lambda/A}/f$ in conventional DFS.[26]

If A is comparable to λ_a, as in the example under discussion, only few harmonics F_m are significant,[25] but many low-frequency harmonics with measurable intensities R_i nevertheless arise as long as the peak-to-peak amplitude $2A_Z$ covers the range of strong $\Delta f(Z)$ variations. A larger modulation amplitude would not be much help because it would yield almost constant contributions to the lowest R_i from short-range forces. Most of their i dependence would arise from long-range forces, which contribute alone once Z_c lies in the tail of $\Delta f(Z)$. Being site-independent, the latter could in practice be preferably determined in a single direct measurement between one and a few nanometers[27] and smoothly matched to the output of our reconstruction procedure. Useful information about the distance dependence $\Delta f(Z)$ is contained in the Fourier components R_i, which are not too small. In Fig. 1(c), the intensity of the 12th harmonic is already less than 1% of the first harmonic. Therefore, keeping only the lowest 12 peaks in the frequency spectrum might be sufficient to reconstruct the distance dependence of Δf. The $\Delta f(t)$ signal also contains a DC (time-averaged) component, which can be calculated as $\overline{\Delta f}(Z_c) = 1/\pi \int_0^{\pi} \Delta f[Z_c + A_Z(1+cos\theta)]d\theta$. Figure 1(d) shows the distance dependence of $\overline{\Delta f}(Z_c)$. Since $A_Z = 500$ pm is larger than λ_a, the most negative $\overline{\Delta f}(Z_c)$ is closer to the sample surface than for $\Delta f(Z)$. This beneficial effect allows one to set Z_c close enough to detect atomic-scale contrast while scanning the surface using small resonance oscillation amplitude $A = 100$ pm on the positive slope branch of $\overline{\Delta f}(Z_c)$, where DFM is usually performed.[18]

The real-time signal reconstructed from the truncated Fourier series,

$$\Delta f(t) = \overline{\Delta f}(Z_c) + \sum_{i=1}^{n} R_i \cos(2\pi i f_Z t + P_i), \quad (2)$$

can be compared to the actual one in Fig. 1(a). Here, R_i is the amplitude and P_i the phase calculated from the real and imaginary components of the ith complex Fourier coefficient of the actual $\Delta f(t)$ signal determined from the FFT. Without force hysteresis between approach and retraction swings, the phase of the ith harmonic in the FFT spectrum is 0° or 180°. Figure 1(e) shows reconstructed real-time Δf signals keeping harmonics up to 6th, 12th, and 18th order from the spectrum in Fig. 1(c). The reconstruction up to 6th order is not satisfactory because unphysical oscillations (Gibbs phenomenon) appear, especially whenever the actual signal is flat. However, since no significant differences are observed between reconstructed signals cut off at the 12th and 18th orders, the inclusion of harmonics up to the 12th order is adequate enough to faithfully reconstruct the real-time signal. Furthermore, since the tip-sample distance is sinusoidally modulated over the range where Δf varies appreciably, its distance dependence can easily be extracted from the corresponding reconstructed $\Delta f(t)$ signal, as illustrated in Fig. 1(f). The remarkable agreement between the original [Fig. 1(a)] and reconstructed [Fig. 1(f)] curves, keeping harmonics up to 12th order, unambiguously illustrates the validity of our approach.

III. EXPERIMENTAL

All experiments were performed with an in-house built atomic force microscope, operating at RT in UHV.[28] The clean KBr(001) sample was obtained by cleaving in UHV, and subsequent annealing at 200 °C for removing residual charges. A commercially available stiff Si cantilever (Nanosensors: NCL-PPP) was used as a force sensor. Contamination, such as water, was removed by annealing at 150 °C in UHV and the tip was then cleaned by Ar^+ sputtering. In all measurements, the second flexural resonance mode was used to realize a small amplitude operation thanks to its high effective stiffness ($k_{2nd} \approx 1400$ N/m).[27] Setting a small amplitude $A \sim 100$ pm is important to optimize the signal-to-noise ratio in DFS.[29,30] Two sets of commercially available multiple digital lock-in amplifiers were employed to realize a synchronous detection of 12 harmonic signals,[31] each set containing six lock-in amplifiers.

Figure 2 shows a schematic diagram of the measurement setup. The motion of the cantilever, self-driven on the shifted resonance of the second flexural mode, is sensed by the beam deflection detector. The photodetector signal is fed into a digital circuit, which includes a digital phase-locked loop that accurately tracks the resonance frequency and provides the driving signal to the dither piezo-actuator. The excitation amplitude is continuously adjusted to keep constant the tip oscillation amplitude A. A sinusoidal signal with a frequency $f_Z = 46$ Hz is added to the Z scanner control voltage which keeps constant the DC component $\overline{\Delta f}(Z_c)$ like in conventional frequency-modulation DFM. The feedback gain of the Z controller is set weak, so that the tip-sample distance is modulated over $2A_Z = 1$ nm. The resonance frequency caused by the tip-sample interaction, is therefore modulated as the tip apex swings toward and away from the sample surface. In order to faithfully detect all sidebands up to 12th order, the bandwidth of the PLL was set to $B = 1000$ Hz. Owing to the self-driven excitation scheme, the resonance and sideband peaks are much narrower than the resonance of the freely oscillating cantilever.[18] The demodulated 12 harmonic

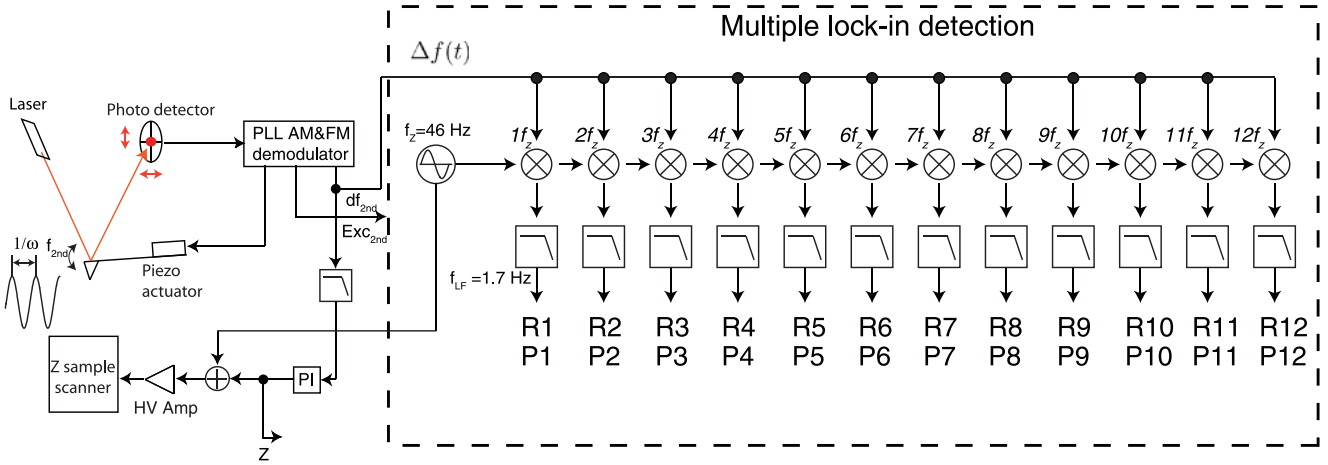

FIG. 2. (Color online) Schematic diagram of the measurement setup based on the multiple lock-in technique.

components of $\Delta f(t)$ are simultaneously detected by the multiple lock-in amplifiers as illustrated in Fig. 2, each equipped with a low-pass filter with a cutoff frequency $B_{\rm LF} = 1.7$ Hz. This filtering ensures that only spectral components very close to the harmonic frequencies are detected. $B_{\rm LF}$ is narrow enough to avoid cross talk from neighboring harmonics. Since noise is collected within $\pm B_{\rm LF}$ of each harmonic of f_Z, the effective bandwidth for the reconstructed $\Delta f(Z_c)$ is thus 3.4 Hz $\times$ 12. As shown in Sec. IV, 12 harmonics indeed adequately represent $\Delta f(Z_c)$ in the chosen sweep range. Therefore, it makes sense to compare the quoted measurement bandwidth with a hypothetical direct recording of $\Delta f(Z_c)$ at a sweep rate of 1.7 Hz. In order to collect the information contained in 12 harmonics of that frequency, the PLL bandwidth would have to be set above 12×1.7 Hz. At first glance, one might think that the conventional method is better due to the halved measurement bandwidth. But the crucial advantage of the current lock-in-based approach is that the noise collected within ±1.7 Hz of most harmonics of f_Z is white, whereas in the corresponding conventional measurement mostly $1/f$ noise would be collected. In order to reduce the signal-to-noise ratio in actual conventional measurements, the sweep rate is therefore set lower. In other words, the recording time at each discrete separation Z_c is longer, so that the measurement becomes distorted by nonlinear drifts. Such drifts can be largely compensated, albeit at the cost of additional time for tip-repositioning by "atom-tracking" between successive records.[9,10]

Since $\overline{\Delta f}(Z_c)$ is kept constant, $1/f$ noise in that quantity and in Z_c is averaged over the whole measurement time. On the other hand, since the low-pass filtering is limited to 1.7 Hz, the detected harmonic signals are averaged over the $46/1.7 \approx 27$ Z modulation cycles and more rapid events, such as tip and/or surface configurational changes, cannot be resolved, although they affect the instantaneous force $F[z(t)]$, and hence its average distance dependence and that of the measured $\Delta f(Z_c)$.[5,32]

IV. RESULTS AND DISCUSSION

In order to provide a comparison with Fig. 1(c), Fig. 3(a) shows examples of power spectral densities of $\Delta f(t)$ obtained from a FFT, sampled at 500 Hz of the phase-locked loop output at three distinct atomic sites. Site-dependent peaks at harmonics of f_Z are clearly observed and their heights tend to decrease with increasing harmonic order. Nevertheless, a nonmonotonic evolution is apparent beyond the 7th order peak. The topographic image, composed of 128×128 pixels as shown in Fig. 3(b), was taken at constant time-averaged $\overline{\Delta f}$ of -120 Hz, while modulating the tip-sample distance. In order to avoid any resonance of the Z distance control circuit by the modulation signal, the feedback gains were intentionally set at weak levels, so that the measured corrugation amplitude is rather small (<29 pm), while still being large enough to show atomic-scale resolution. Maps of the harmonic signal intensities R_i were simultaneously recorded with the 12 lock-in amplifiers. As shown in Fig. 3(c), clear atomic-scale contrast is observed in all R_i maps, except when the noise level is approached. The mean value of the R_1 map is approximately 93.3 Hz and the relative magnitude of the R_{12} signal is less than 1.2%. In contrast to conventional 3D-DFS, no atom-tracking was necessary, and the residual X and Y thermal drifts were corrected *a posteriori*, taking into account the surface periodicity. One set of forward and backward frames like that in Fig. 3(b) took 1285 s, so that the corresponding recording time for the cut-out images with an area of 870 $\times$1160 pm, displayed in Fig. 3(c), was approximately 400 s.

We generated a 3D-$\Delta f(x,y,z)$ dataset from the harmonic intensity maps. At each (x,y) pixel, the 12 recorded R_i values are inserted into Eq. (2) and the distance dependence of the reconstructed Δf is calculated *a posteriori* at each pixel, as illustrated in Fig. 4(a). Owing to unavoidable phase delays of the PLL circuit and the sample Z scanner, the phases of the harmonic Δf signals are not exactly 0° or 180°. However, the delays are small enough to set each P_i equal to one of those values, so that the reconstructed $\Delta f(Z_c)$ correspond to the total force averaged over $f/B_{\rm LF} \sim 5 \times 10^5$ cantilever oscillations. Figure 4(b) shows a series of constant height images at different tip-sample distances extracted from cuts through the reconstructed 3D-Δf data. As observed, atomic-scale corrugation is resolved in all images. As previously observed in drift-corrected 3D Δf maps,[10] clear shifts of the

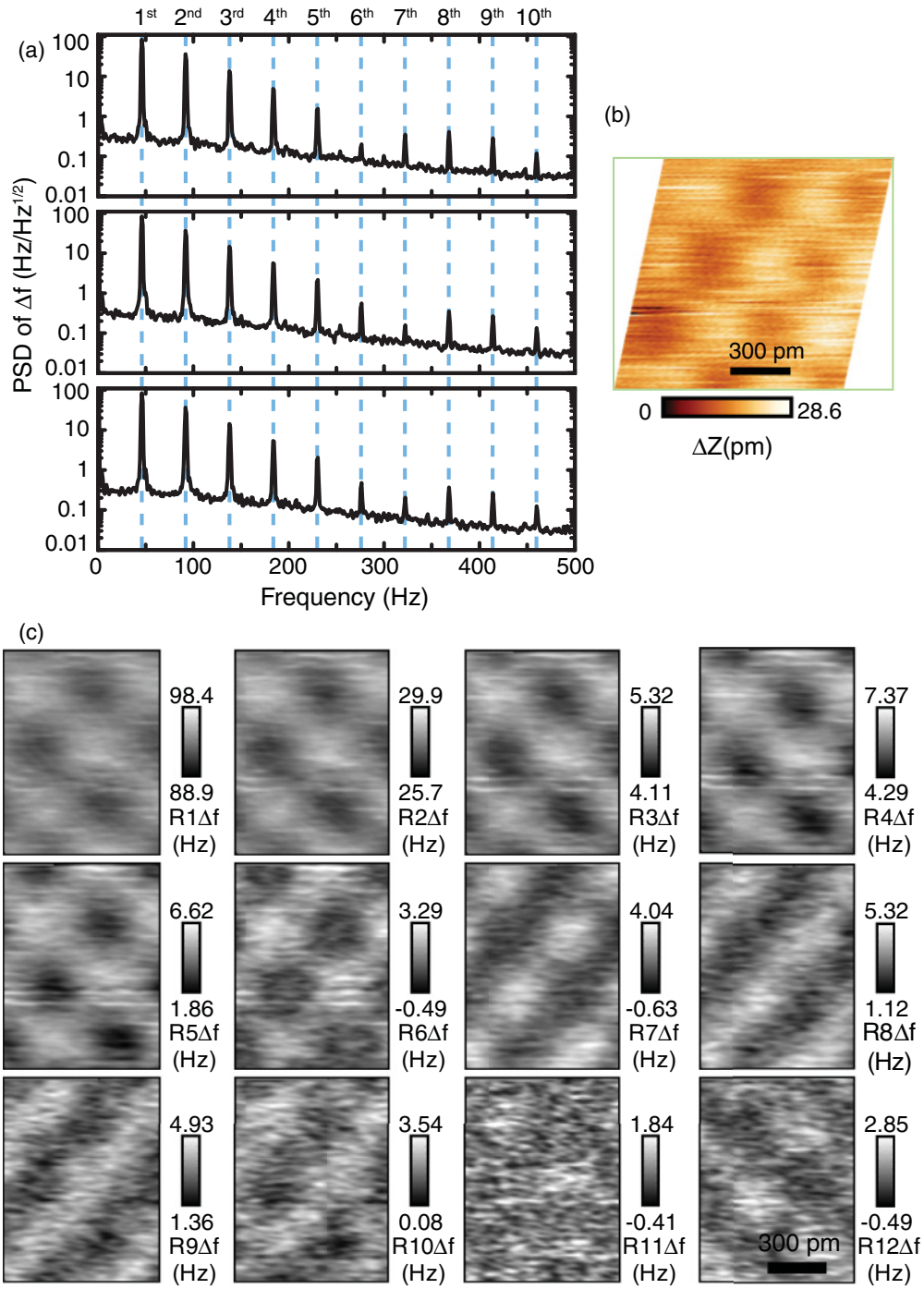

FIG. 3. (Color online) (a) Examples of power spectral densities of the modulated resonance frequency $\Delta f(t)$ at three different atomic sites on KBr(001). (b) Topographic image obtained at a constant time-averaged $\overline{\Delta f} = -120$ Hz. (c) Series of 12 harmonic intensity maps simultaneously recorded while scanning the surface. Imaging parameters: $A_{2nd} = 100$ pm; $f_{2nd} = 1011520$ Hz; $Q_{2nd} = 17920$; $V_{bias} = 0$ V; $f_Z = 46$ Hz; and $A_Z = 500$ pm.

lattice of maxima and minima by up to half a lattice spacing, which can be attributed to tip and/or sample deformations, are observed.

V. CONCLUSIONS AND OUTLOOK

In summary, by using multiple lock-in amplifiers, we proposed and successfully tested a rapid method for reconstructing the distance dependence of the resonance frequency shift induced by forces acting on the probe tip of an atomic force microscope. A high-resolution 3D-Δf dataset above a KBr(001) surface with an area of 870 $\times$1160 pm was obtained in 400 s. Compared to our previous measurement using drift-corrected 3D mapping[10] within an area of 700 $\times$700 pm, which took 23 h and 34 min, the measurement speed was faster by a factor of 210. It is worth noting that the pixel density of

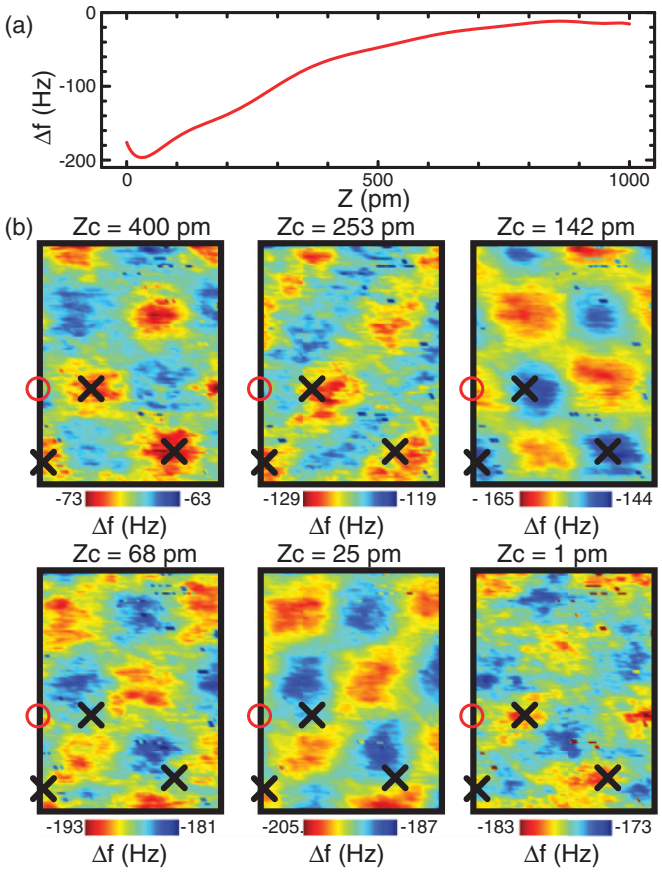

FIG. 4. (Color online) (a) Reconstructed 1D-Δf vs. distance curve at a particular site. (b) Constant height images of Δf extracted from the reconstructed 3D-Δf dataset at different Z_c. The location of (a) is indicated by circles in (b). The cross markers indicate reference points.

the cut-out images in the present work (85×109) is higher than in the previous work (71×71), while the signal-to-noise ratio is less but still high enough to recognize systematic pattern shifts caused by deformations of the tip and/or sample. Taking into account the spatial and force resolution, the total resolution in the two measurements would be comparable. We believe that this method can be generally applied, not only for scanning probe measurements but also to the measurements of any single-valued physical quantity with a smooth but strong nonlinear dependence on a control variable.

Important next steps would be to determine optimal measurement parameters for generating strong harmonics of the $\Delta f(t)$ signal and to relate the dependence of their intensities R_i to different kinds of tip-sample interactions. Thus, by analogy with the discussion of Fig. 1(c), the nonmonotonic variation of the spectral peaks beyond 7th order in Fig. 3(a) suggests that a weak repulsive interaction is already noticeable at the chosen Z_c, which, according to Fig. 4(a), is near the negative minimum of Δf. Furthermore, the more gradual variations of the peak intensities in the experimental spectrum indicate appreciable deviations from the Morse potential model, which may be due to induced displacements of tip and sample atoms at short distances.[3,20]

In the case of an ultrasmall resonance amplitude ($A <$ 50 pm in practice), this position would coincide with that of the maximum force gradient F' because $\Delta f/f \simeq -F'/(2k)$ in that limit.[18] Harmonics of the $\Delta f(t)$ signal would then probe the nonlinearity of the force gradient over the distance modulated by the Z scanner. At a given distance close to the surface, the force gradient is more sensitive to short-range interactions than the force itself. Motivated by theoretical work by Dürig,[25] Hembacher *et al*. pointed out that higher harmonics of the *cantilever deflection* were even more sensitive to such interactions and reported a rather different measurement on the Graphite(0001) surface.[33] They detected the total rms amplitude of the high-pass filtered part of the deflection signal using a filter cutoff slightly above the resonance frequency $f \simeq 18$ kHz of the tuning fork sensor, which they used instead of a cantilever. The detected signal was therefore a sum over higher harmonics $mf (m > 1)$, which are excited by the nonlinearity of the tip-sample interaction *force* and are predicted to be significant if the oscillation amplitude A is comparable to the interaction range.[25] In principle, the physical content of the signals probed in both measurements is the same but, being based on an additional low-frequency modulation, the present measurement has the advantage of generating many relevant harmonics within the bandwidth of the frequency detector which are individually measured without appreciable distortion. In the present work, the chosen amplitude $A = 100$ pm is not small enough to directly probe the tip-sample force gradient. Nevertheless, it is interesting that both bridge- and ball-like atomic contrast patterns, perhaps due to unresolved tip changes,[34] can be observed in the higher harmonic R_i maps [Fig. 3(c)].

So far, we only considered conservative tip-sample interactions. Dissipative tip-sample interactions that can be detected via the variations of the excitation amplitude required to keep constant the tip resonance amplitude A (Ref. 35) are often observed at the distances where atomic-scale contrast appears. If our method were used to simultaneously detect higher harmonics of the excitation amplitude, then the reconstruction of the distance dependence of the interaction-induced energy dissipation might in principle also be possible. If an additional low-frequency tip-sample distance modulation is applied, dissipation may cause the phases P_i in Eq. (2) to significantly deviate from 0° or 180°. In particular, it is worth noting that if the peak-to-peak amplitude $2A$ becomes smaller than the width of a distinct force hysteresis loop in the interval $Z_1 < Z_2$ due, e.g., to atomic-scale rearrangements,[36] a hysteresis loop should also become directly observable between distinct $\Delta f(Z_c)$ curves in the same range upon approach and retraction of the oscillating cantilever. The phases P_i would then systematically change, depending on whether the additional Z modulation encompasses this hysteresis loop or not.

ACKNOWLEDGMENTS

This work was supported in part by the Swiss National Science Foundation, the ESF EUROCORE programme FANAS and by the NCCR "Nanoscale Science" of the Swiss National Science Foundation. S.K. thanks Christoph Werle for the helpful discussions.

*shigeki.kawai@unibas.ch

[1] R. L. Schwoebel and E. J. Shipsey, J. Appl. Phys. **37**, 3682 (1966).

[2] H. Hölscher, D. Ebeling, and U. D. Schwarz, Phys. Rev. Lett. **101**, 246105 (2008).

[3] M. A. Lantz, H. J. Hug, R. Hoffmann, P. J. A. van Schendel, P. Kappenberger, S. Martin, A. Baratoff, and H. J. Güntherodt, Science **291**, 2580 (2001).

[4] Y. Sugimoto, P. Pou, M. Abe, P. Jelinek, R. Pérez, S. Morita, and O. Custance, Nature (London) **446**, 64 (2007).

[5] S. Kawai, F. F. Canova, T. Glatzel, A. S. Foster, and E. Meyer, Phys. Rev. B **84**, 115415 (2011).

[6] M. Ternes, C. P. Lutz, C. F. Hirjibehedin, F. J. Giessibl, and A. J. Heinrich, Science **319**, 1066 (2008).

[7] L. Gross, F. Mohn, N. Moll, P. Liljeroth, and G. Meyer, Science **325**, 1110 (2009).

[8] B. J. Albers, T. C. Schwendemann, M. Z. Baykara, N. Pilet, M. Liebmann, E. I. Altman, and U. D. Schwarz, Nat. Nanotechnol. **4**, 307 (2009).

[9] M. Abe, Y. Sugimoto, O. Custance, and S. Morita, Appl. Phys. Lett. **87**, 173503 (2005).

[10] S. Kawai, T. Glatzel, S. Koch, A. Baratoff, and E. Meyer, Phys. Rev. B **83**, 035421 (2011).

[11] T. Fukuma, Y. Ueda, S. Yoshioka, and H. Asakawa, Phys. Rev. Lett. **104**, 016101 (2010).

[12] J. B. Johnson, Phys. Rev. **26**, 71 (1925).

[13] M. L. Meade, *Lock-In Amplifiers: Principles and Applications (IEE Electrical Measurement Series)* (P. Peregrinus, London, 1983).

[14] S. Kitamura and M. Iwatsuki, Appl. Phys. Lett. **72**, 3154 (1998).

[15] Y. Sugimoto, T. Namikawa, M. Abe, and S. Morita, Appl. Phys. Lett. **94**, 023108 (2009).

[16] C. Hutter, D. Platz, E. A. Tholén, T. H. Hansson, and D. B. Haviland, Phys. Rev. Lett. **104**, 050801 (2010).

[17] E. A. Tholén, D. Platz, D. Forchheimer, V. Schuler, M. O. Tholén, C. Hutter, and D. B. Haviland, Rev. Sci. Instrum. **82**, 026109 (2011).

[18] T. R. Albrecht, P. Grütter, D. Horne, and D. Rugar, J. Appl. Phys. **69**, 668 (1991).

[19] F. J. Giessibl, Phys. Rev. B **56**, 16010 (1997).

[20] R. Pérez, I. Štich, M. C. Payne, and K. Terakura, Phys. Rev. B **58**, 10835 (1998).

[21] M. Guggisberg, M. Bammerlin, C. Loppacher, O. Pfeiffer, A. Abdurixit, V. Barwich, R. Bennewitz, A. Baratoff, E. Meyer, and H. J. Güntherodt, Phys. Rev. B **61**, 11151 (2000).

[22] S. Kawai, T. Glatzel, S. Koch, B. Such, A. Baratoff, and E. Meyer, Phys. Rev. Lett. **103**, 220801 (2009).

[23] J. R. Lozano and R. García, Phys. Rev. Lett. **100**, 076102 (2008).

[24] S. Kawai, T. Glatzel, S. Koch, B. Such, A. Baratoff, and E. Meyer, Phys. Rev. B **81**, 085420 (2010).

[25] U. Dürig, New J. Phys. **2**, 5 (2000).

[26] A. Abdurixit, A. Baratoff, and E. Meyer, Appl. Surf. Sci. **157**, 355 (2000).

[27] S. Kawai, T. Glatzel, S. Koch, B. Such, A. Baratoff, and E. Meyer, Phys. Rev. B **80**, 085422 (2009).

[28] L. Howald, E. Meyer, R. Lüthi, H. Haefke, R. Overney, H. Rudin, and H. J. Güntherodt, Appl. Phys. Lett. **63**, 117 (1993).

[29] F. J. Giessibl, H. Bielefeldt, S. Hembacher, and J. Mannhart, Appl. Surf. Sci. **140**, 352 (1999).

[30] S. Kawai, S. Kitamura, D. Kobayashi, S. Meguro, and H. Kawakatsu, Appl. Phys. Lett. **86**, 193107 (2005).

[31] Zurich Instruments AG, HF2LI and HF2-PLL options, Zurich, Switzerland, [http://www.zhinst.com/].

[32] S. A. Ghasemi, S. Goedecker, A. Baratoff, T. Lenosky, E. Meyer, and H. J. Hug, Phys. Rev. Lett. **100**, 236106 (2008).

[33] S. Hembacher, F. J. Giessibl, and J. Mannhart, Science **305**, 380 (2004).

[34] A. S. Foster, C. Barth, A. L. Shluger, and M. Reichling, Phys. Rev. Lett. **86**, 2373 (2001).

[35] B. Anczykowski, B. Gotsmann, H. Fuchs, J. P. Cleveland, and V. B. Elings, Appl. Surf. Sci. **140**, 376 (1999).

[36] N. Sasaki and M. Tsukada, Jpn. J. Appl. Phys. **39**, L1334 (2000).